A NEW MODIFIED WAVELET-BASED ECG DENOISING

CONCORDIA UNIVERSITY

Sepehr Ghamari
Arman Bakhtiari

December 6, 2023

Abstract: The paper presents an innovative approach to ECG signal denoising, utilizing a newly developed wavelet method. The research focuses on improving the denoising process by designing a modified wavelet filter, specifically for ECG signals. This filter is optimized to closely approximate the ideal filter's amplitude-frequency response, thereby enhancing the denoising efficacy while preserving ECG signal prominent features. Extensive testing on clinical ECG data and simulated atrial fibrillation signals demonstrates the superiority of this method over traditional wavelet techniques like db4 and Sym4. At the end of this project our results from a similar implementation has been provided.

1. INTRODUCCIÓN

The electrocardiogram (ECG) plays a crucial role in medical diagnostics, offering essential insights into the heart's electrical activity, aiding in the detection of abnormalities and contributing to accurate health assessments AlMahamdy and Riley, 2014. However, ECG signals are susceptible to inherent noise, posing challenges in precise signal interpretation and potentially impacting the diagnosis of cardiac conditions AlMahamdy and Riley, 2014. Noise sources such as baseline wander, powerline interference, electromyographic (EMG) noise, and electrode motion artifact noise contribute to the complexity of noise in ECG signals Marzog et al., 2022. Addressing these diverse noise components is essential for successful denoising strategies in ECG signal processing.

Different denoising methods, including Empirical Mode Decomposition (EMD) and deep-learning-based autoencoder models (DAEs), come with specific drawbacks Shi, 2022. For instance, EMD may exhibit sensitivity to noise, and DAEs might face challenges related to extensive training data and potential overfitting. Additionally, the computational complexity of adaptive filtering using Bayesian filters, like the extended Kalman filter, may be high, impacting real-time applications Shi, 2022. The wavelet transform is favored for ECG signal processing due to its excellent time-frequency localization and multi-resolution properties, effectively capturing both high and low-frequency components for denoising tasks Shi, 2022.

However, challenges arise in the selection of an appropriate mother wavelet, impacting the effectiveness of the wavelet transform. Daubechies wavelets, though widely used, may introduce potential boundary effects, especially at signal edges due to finite support. Symlet wavelets aim to address these effects but may introduce oscillations in the reconstructed signal. Furthermore, wavelets designed for orthogonality and symmetry may risk blurring and weakening crucial cardiac signals like P waves and T waves during denoising, particularly in the context of atrial fibrillation (AF) signals. This emphasizes the need for careful consideration of wavelet characteristics and potential trade-offs in denoising applications.

To address these challenges, the paper proposes a modified wavelet design approach, optimizing filter coefficients to achieve an almost symmetric orthogonal wavelet for effective ECG signal denoising.

2. Wavelet Transform

The wavelet transform constitutes a groundbreaking mathematical methodology that revolutionizes signal processing by unveiling the intricate interplay of time and frequency components within a signal. At the heart of this transformative approach lies the Continuous Wavelet Transform (CWT), expressed as:

$$CWT(a,b) = \int_{-\infty}^{\infty} x(t)\Psi_{a,b}^{*}(t)\,dt \qquad (1)$$

Here, $x(t)$ represents the signal under examination, and $\Psi_{a,b}(t)$ stands for the mother wavelet function, with a and b as the scale and translation parameters. This formulation captures the essence of the wavelet transform, emphasizing its capacity to dissect a signal into its constituent components at varying scales and time points.

The Discrete Wavelet Transform (DWT), a discrete counterpart to the CWT, introduces a discrete set of scales and translations, making it computationally efficient for digital signal processing. The DWT is represented as:

$$\mathrm{DWT}(j,k) = \sum_{n} x(n)\psi_{j,k}(n) \qquad (2)$$

In this formula, $x(n)$ is the discrete signal, and $\psi_{j,k}(n)$ is the discrete wavelet function. The DWT facilitates multiresolution analysis and has widespread applications in signal compression and feature extraction.

Pioneering work by Mallat, 1989. 1 laid the theoretical foundation for multiresolution signal decomposition, setting the stage for the widespread adoption of wavelet transforms. This mathematical elegance allows researchers and practitioners to delve into the fine details of signals, uncovering nuances that might be obscured in traditional Fourier-based analyses.

2.1. Applications in Image Processing

Beyond its mathematical elegance, the wavelet transform has found profound applications in the field of image processing, fundamentally altering how we analyze and manipulate visual information. One of the pivotal contributions comes from the work of Shapiro, 1993, whose pioneering efforts in embedded image coding using zerotrees of wavelet coefficients marked a transformative moment in image compression.

The wavelet transform's unique ability to capture both local and global variations within an image makes it particularly well-suited for tasks such as image compression. Unlike traditional methods like Fourier transforms, which might struggle with representing localized features, wavelets excel at preserving intricate details across different scales. This is crucial in scenarios where preserving fine details is paramount, such as in medical imaging or satellite imagery.

The concept of zerotrees introduced by Shapiro involves efficiently encoding wavelet coefficients based on their significance, leading to highly effective compression algorithms. By exploiting the sparsity inherent in many natural images, wavelet-based compression techniques can achieve high compression ratios without sacrificing essential visual information. This is of paramount importance in applications like digital photography, where minimizing file sizes while retaining image quality is a constant pursuit.

Moreover, wavelet-based denoising techniques have become instrumental in enhancing the quality of images. The multiresolution analysis offered by wavelets allows for the identification and removal of noise at different scales, leading to cleaner and more visually appealing images. This is particularly beneficial in fields such as medical imaging, where the clarity of diagnostic images is crucial.

In recent years, wavelet transforms have also played a significant role in image fusion, where information from multiple images is combined to create a composite image with enhanced features. This has applications in fields ranging from surveillance to remote sensing, where combining visual data from different sources can provide a more comprehensive understanding of a scene.

The adaptability of wavelet transforms in image processing extends beyond compression and denoising. Its ability to efficiently represent and analyze image features at various scales has opened avenues for advanced image recognition and computer vision applications. This includes object detection, facial recognition, and even artistic style transfer, where the unique capabilities of wavelets contribute to pushing the boundaries of what is achievable in visual information processing.

2.2. Biomedical Signal Processing

In the complex domain of biomedical signals, the wavelet transform emerges as a versatile tool. The

work of Schomer, 2011 in Electroencephalography: Basic Principles, Clinical Applications, and Related Fields underscores the adaptability of wavelet transforms in extracting meaningful information from electroencephalograms (EEG). By seamlessly capturing both temporal and frequency intricacies, the wavelet transform proves indispensable for discerning patterns in complex biological signals.

In essence, the wavelet transform transcends the confines of traditional signal processing, providing a dynamic lens through which signals can be scrutinized at various scales and time points. This ability to unravel the inherent complexity of signals positions the wavelet transform as a cornerstone in modern signal processing, enabling advancements across a spectrum of scientific disciplines.

3. Image Denoising Using Wavelet Transform

Image denoising, a critical aspect of image processing, aims to remove unwanted noise from images while preserving essential details. Among various techniques, the application of wavelet transform in image denoising has proven to be highly effective. The unique multiresolution analysis capabilities of wavelets allow for targeted noise reduction at different scales, contributing to visually clearer and more refined images. The application of wavelet transform in image denoising encompasses a well-defined algorithm, as illustrated in Figure 1.

The wavelet denoising algorithm consists of three key steps: wavelet decomposition, coefficient processing, and wavelet reconstruction. In the process of wavelet decomposition, two-scale equations facilitate the dilation and translation of time, yielding scale coefficients and wavelet coefficients at various scales. The Fourier transform of the scaling function and the wavelet function exhibits low-pass and high-pass filtering properties, respectively. The Mallat algorithm Mallat, 1989 enables the realization of wavelet transform and denoising, as depicted in Figure 1. Here, 'S' represents the input signal, while 'H(n)' and 'G(n)' denote low-pass and high-pass filters, forming a dual-channel filter bank. The coefficients 'h(n)' and 'g(n)' are determined by the scaling and wavelet functions.

In the coefficient processing step, the threshold is estimated based on the characteristics of EMG noise. This threshold is then applied to handle the decomposed wavelet coefficients effectively.

The final step involves wavelet reconstruction, where the processed wavelet coefficients undergo reconstruction using mirror filters. The result is a denoised ECG signal, preserving essential features while mitigating the impact of noise. the advantages of wavelet-based denoising lie in its ability to perform adaptive, multiresolution analysis, retaining important image features while effectively reducing noise. This makes it a powerful and widely applicable technique in diverse image-processing scenarios.

While wavelet-based denoising offers significant advantages, choosing an appropriate threshold and wavelet function is crucial. Different types of wavelet functions, such as Daubechies or Symlet, may have distinct effects on denoising performance. Additionally, the threshold value requires careful consideration to balance noise reduction and feature preservation.

In conclusion, image denoising using wavelet transform provides a powerful and versatile approach to enhance visual clarity in images. The combination of mathematical precision and adaptive noise reduction makes wavelet-based denoising a valuable tool in diverse fields, from medical imaging to improving the quality of digital photographs.

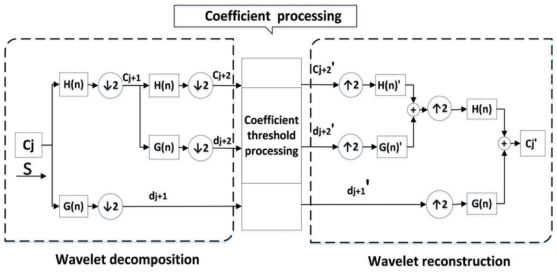

Figure 1: *Schematic diagram of wavelet denoising algorithm*

4. Methodology

The proposed wavelet denoising process for ECG signals, involves a three-step algorithm: wavelet decomposition, coefficient processing, and wavelet reconstruction. This process is illustrated in Figure 1 and its methodology is rooted in the principles of wavelet theory, particularly the use of two-scale equations and the Mallat algorithm Mallat, 1989. During wavelet decomposition, the two-scale equations enable the dilation (scaling) and translation (shifting) of the time domain, allowing the analysis of the ECG signal across various scales. This step breaks down the signal into its frequency components. Through this process, two types of coefficients are obtained: scale coefficients,

representing the low-frequency content, and wavelet coefficients, representing the high-frequency content. The Fourier transform is applied to both the scaling and wavelet functions. The scaling function acts as a low-pass filter, while the wavelet function serves as a high-pass filter. As mentioned before the Mellat algorithm has been used for the decomposition and reconstruction of the signal. In this algorithm (Figure 1), the ECG signal 'S' is processed through a pair of mirror filters forming a dual-channel filter bank: 'H(n)' for low-pass filtering and 'G(n)' for high-pass filtering. The coefficients 'h(n)' and 'g(n)' of these filters are derived from the scaling and wavelet functions, respectively. The decomposed signal then goes through a coefficients processing which involves estimating a threshold based on the characteristics of the noise present in the ECG signal, such as EMG noise, a common type of noise in ECG signals, can overlap with the frequency components of the ECG signal. This threshold distinguishes between the noise and the actual ECG signal within the wavelet coefficients by reducing coefficients that are more likely to represent noise than the signal. This process preserves the integrity and important features of the ECG signal, such as the P wave, QRS complex, and T wave.

The final step involves reconstruction of the ECG signal from the processed wavelet coefficients. This reconstruction is achieved through the inverse application of the wavelet transform, using the mirror filters. The outcome is a denoised ECG signal where the essential features are preserved, but the noise is substantially reduced or removed.

4.1. Modified wavelet design

The concept of an ideal filter in signal processing is theoretically perfect. It would allow for the absolute separation of desired signal components from unwanted noise, achieving zero frequency components in the stopband without any loss or distortion in the passband. However, in practical scenarios, this level of perfection is not achievable due to inherent physical and computational limitations. One significant challenge is aliasing, causing different signal frequencies to become indistinguishable. When decomposing signals into multiple frequency bands using a non-ideal filter, aliasing can lead to a distortion where the characteristic information of the signal is weakened or lost, especially in overlapping frequency bands. Figure 2 shows the amplitude-frequency response of different frequency aliasing types.

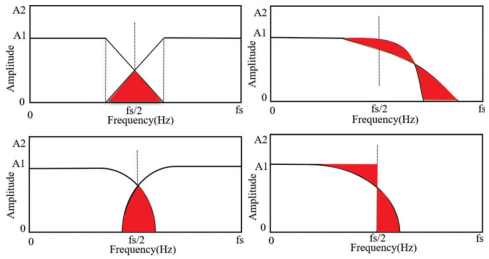

Figure 2: AFR of different frequency aliasing types

To navigate these limitations, the use of optimization techniques has been proposed to approximate the ideal filter as closely as possible. The goal of optimization is to minimize the difference between the amplitude-frequency response of the actual filter and the ideal filter. This approach allows for the construction of a filter that, while not perfect, significantly reduces the effects of aliasing and other distortions. By optimizing the filter coefficients, it is possible to create a wavelet filter that effectively denoises ECG signals, striking a balance between removing noise and preserving essential signal characteristics. Additionally, the use of optimization provided a structured approach to handle the complexities of filter design, such as maintaining orthogonality and symmetry in the wavelet, which are essential for accurate signal reconstruction and phase preservation. Orthogonal wavelets are a type of wavelet where the wavelet and scaling functions form an orthogonal basis. This means that they can decompose a signal into independent, non-overlapping frequency components. By using symmetric coefficients to approximate the ideal filter, we can construct nearly orthogonal wavelets.

The error function proposed in the paper as the objective function is as the equation 3:

$$min\ (Eamp) = min(\sum_{w=0}^{\pi/2}(1-|H(w)|^2)+\sum_{w=\pi/2}^{\pi}(|H(w)|^2) \tag{3}$$

However, it is not easy to solve this minimization problem. Considering the filter has symmetric coefficients and has the length of L, the error function is reformulated to equation 4. This approach simplifies the optimization process and ensures that the filter has a linear phase response.

$$|H(w)|^2 = \frac{1}{2}[|\sum_{n=0}^{L-1} h(n)cos(nw)|^2 + |\sum_{n=0}^{L-1} h(n)sin(nw)|^2] \quad (4)$$

By doing so, the filter's AFR is optimized, and the wavelet designed for denoising becomes nearly orthogonal, which is ideal for accurate signal reconstruction. There is also another constraint applied on the optimization problem which is:

$$\sum_{n=0}^{L-1} h(n) = \sqrt{(2)} \quad (5)$$

This is due to the normalization factor of the two-scale functions. To solve this optimization problem a specific optimization technique known as the trust-region-reflective algorithm has been deployed. This algorithm is a variation of the trust-region method, which is widely used for solving nonlinear optimization problems, particularly those involving multivariate functions. The trust-region-reflective algorithm operates by iteratively refining the solution within a defined region around the current estimate, known as the 'trust region.' Within this region, the algorithm approximates the objective function. The algorithm then updates the solution based on this approximation, expanding or contracting the trust region as needed to ensure convergence towards the optimal solution.

4.2. Realization of modified wavelet

The length of the filter has been assumed to be 8 in the paper. By solving the optimization problem, the coefficients of the optimized filter have been obtained(Table 4.2).

n	$h(n)$
0	0.001590
1	0.056193
2	0.056736
3	0.493436
4	0.493436
5	0.056736
6	0.056193
7	0.001590

Once the coefficients have been achieved the scaling function can be derived by iterative numerical convolution of optimized filter coefficients. Deploying the two-scale functions the wavelet function can be obtained as well. Figure 3 shows the AFR of the scaling and wavelet function.

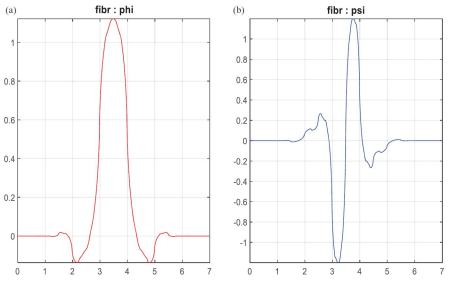

Figure 3: AFR of the scaling and wavelet function

4.3. Denoising evaluation

For the evaluation purposes, the signal to noise ratio (SNR) and the mean squared error (MSE) has been used with the following equations:

$$SNR = 10\log_{(}\frac{\sum_{n=1}^{N} x(n)^2}{\sum_{n=1}^{N}[x(n) - y(n)]^2}) \quad (6)$$

$$MSE = \frac{\sum_{n=1}^{N}[x(n) - y(n)]^2}{N} \quad (7)$$

5. Results

5.1. Data source

The dataset used for testing and validating the proposed methods comprised both normal clinical ECG data and simulated atrial fibrillation (AF) signals. The clinical ECG data were sourced from a standardized database collected and processed by SID Medical Technology Co. Ltd., a company specializing in ECG medical science and technology. This database contains a wealth of diagnostic data derived from consecutive patients treated in the Cardiology Departments of several authoritative hospitals in Shanghai.

In experiments 3.2.1 and 3.2.2, normal ECG data has been used comprising 87 consecutive normal ECG records from the previously mentioned database. Each of these records has a duration of 10 seconds and includes data from 12 leads. The parameters for the acquisition equipment used to record these ECG signals are detailed in Table 5.1.

Parameters	*Values*
Defibrillation protection voltage	5000 V
DC polarization voltage	±300 mV, ±5 %
Frequency response	1–75 HZ, þ0.5 dB, 3.0 dB
Dynamic input range	20 mV
Calibration voltage and accuracy	1 mV, ±5
CMRR□Common mode rejection ratio	>60 dB
System noise	<=15 lV
Nonlinear error	±10
Baseline drift	<=1 mm (5-40 C)
A/D resolution	13 byte, 2.44/bit
Digital sampling rate	500 Hz
Signal length/sampling point	5000

Parameters	*Values*
Frequency, f_0	6 Hz
Frequency variation, Δf	0.2 Hz
Frequency variation frequency, f_f	0.1 Hz
Harmonics, M	3
Amplitude, am [II V1 V5]	[150 75 45]μv
Amplitude variation, Dam [II V1 V5]	[50 25 15]μv
Amplitude variation frequency, fa	0.08 Hz

In experiment 3.2.3, the AF signal has been simulated and used for denoising. The generation method of the F signals is similar to the method used in 'Stridh and Sörnmo, 2001. Table 3 contains the parameters used for generating the F waves.

5.2. Denoising results

5.2.1. Denoising results on normal ECG

For this experiment a White Gaussian Noise (WGN) with the amplitude of 0.3V. To compare the results of the Fibr wavelet, two other wavelets namely Sym4 and db4 wavelets, are also used for the sake of the comparison. Figure 4 shows the SNR and MSE of the signal before denoising (SNR0), and the denoised data employing the three abovementioned wavelets. SNR(i) and MSE(i) where i=0,1,2,3 correspond to the noisy signal, denoised signal using db4, denoised signal using Sym4 and denoised signal using Fibr wavelet respectively. The values in the figure are the average values over the 87 ECG records.

Due to the characteristics of the EMG the level of the decomposition in the denoising algorithm is set to 8, and the threshold is the sure threshold obtained by the unbiased risk estimate of Stein Almahamdy and Riley, 2014.

Figure 5contains the original normal ECG signal, along with noisy signal and the denoised signals using the three wavelets, with respect to time, using II, V1 and V5 leads methods for ECG acquisition. In ECG each lead provides a unique view of the heart, capturing electrical signals from different angles. The leads II, V1, and V5 are part of the standard 12-lead ECG system.

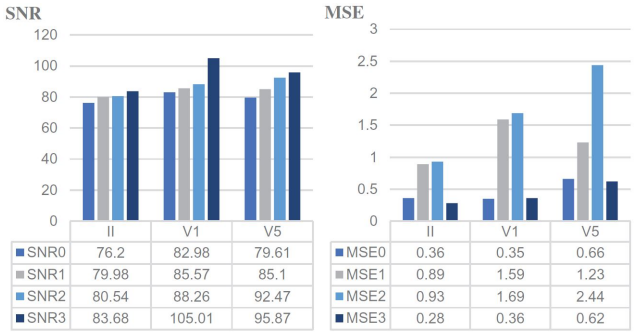

Figure 4: The average denoising effects on normal ECG

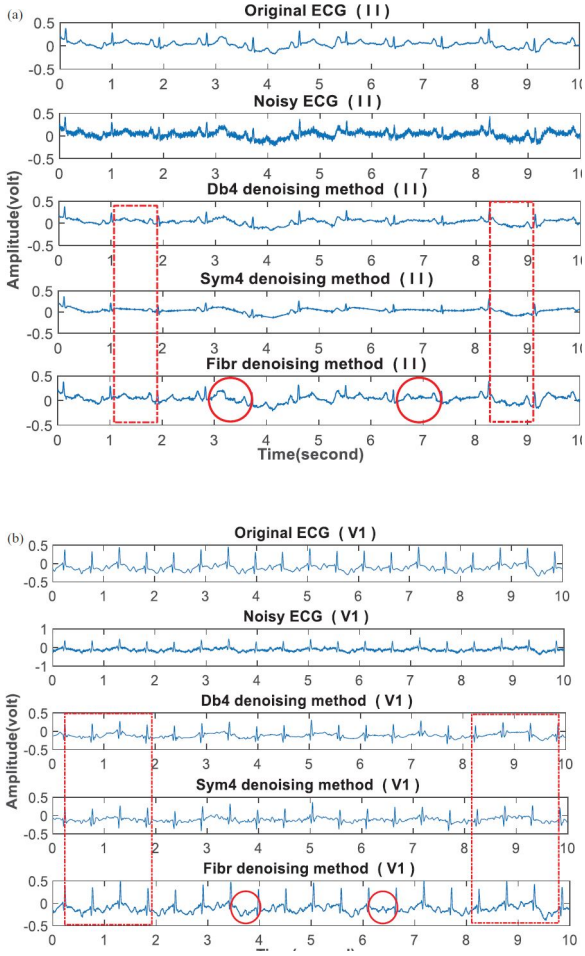

Figure 5: The denoising result on normal ECG. From top to bottom: (a) lead II (b) leadV1 (c) lead V5

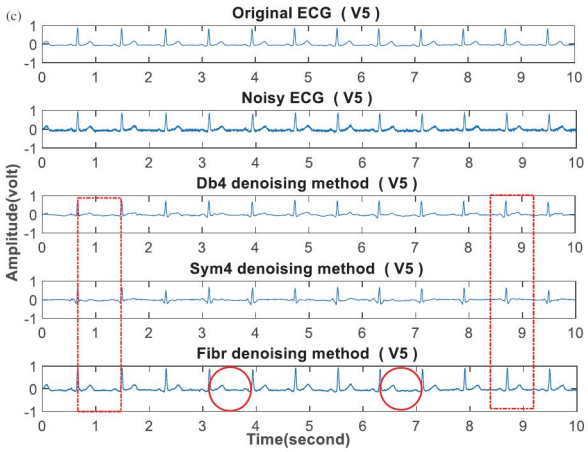

Figure 6: Figure 5 continued.

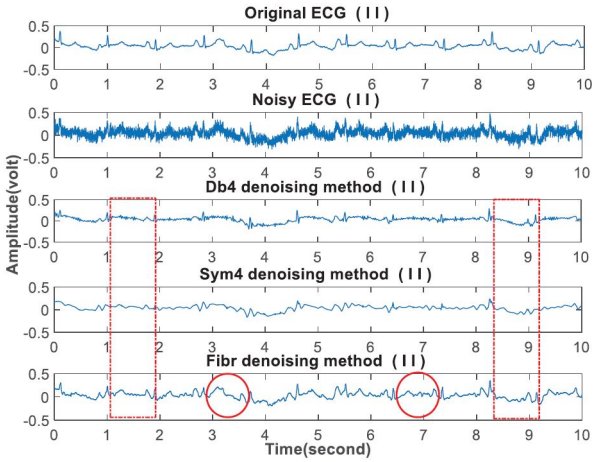

Figure 8: The denoising result under the noise with expected amplitude of 0.065 V

5.2.2. *Denoising results on ECG signals under different noise levels*

In this experiment, the different amplitude of the WGN has been applied on the normal ECG signal (0.015V, 0.03V, and 0.065V). This time only the II lead method is employed for data acquisition. Similar to the previous section the results of the different denoising methods for the WGN of 0.065V amplitude, along with the original and the noisy signal have been provided in Figure 8. Figure 7 also contains the SNR and MSE for different noise amplitudes. As can be seen in both figures, the Fibr wavelet outperforms the other two wavelets. The red circles in Figure 7 show that the Fibr wavelet can reconstruct the P and T waves of the original signal even with the WGN of 0.065V amplitude.

5.2.3. *Denoising results on the simulated AF signals*

For this experiment the F waves are generated according to Table 3, and added to the original signal with a WGN of an amplitude of 0.1mv. Similar to the previous experiments, the average SNR and MSE have been obtained and demonstrated in the Figure 9 using the V5 lead method. Figure 10 also shows the original ECG signal along with the noisy signal and the denoised signal using db4, Sym4 and Fibr wavelet respectively. In this experiment the Fibr wavelet outperforms the two other wavelets again.

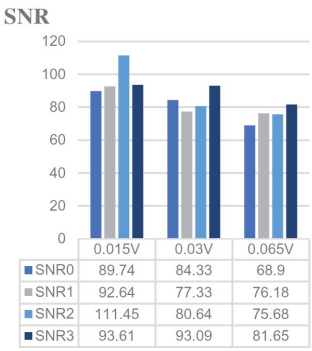

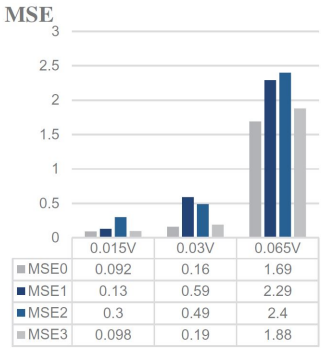

Figure 7: The average denoising effects at different noise levels.

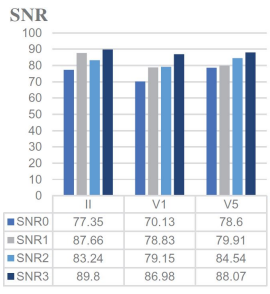

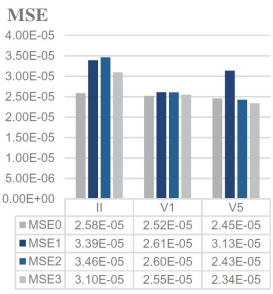

Figure 9: The average denoising effects on simulated AF signals.

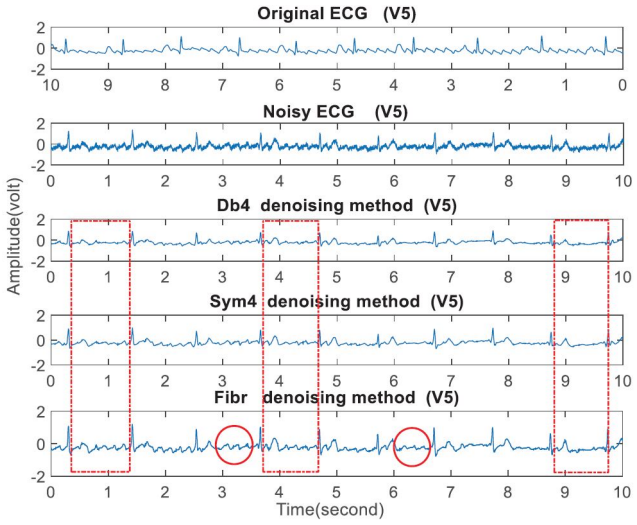

Figure 10: The denoising result on the simulated AF signal

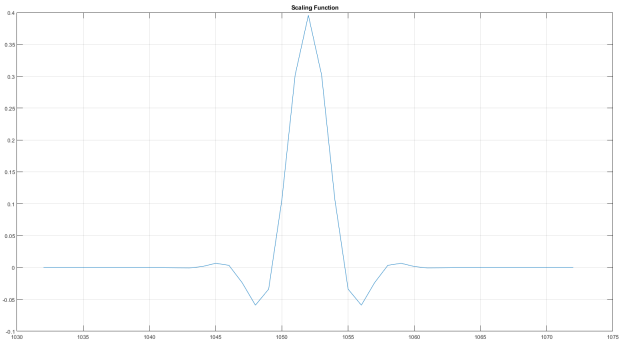

Figure 11: Our Scaling Function

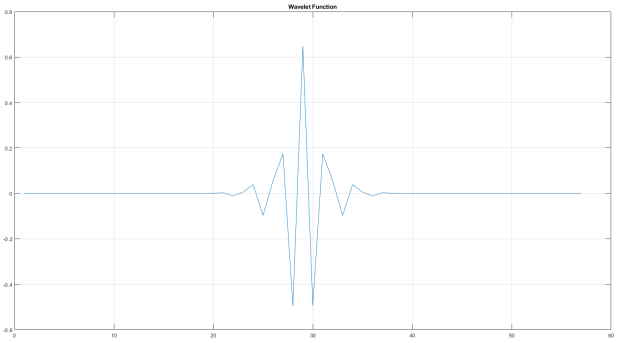

Figure 12: Our Wavelet Function

5.2.4. *Our Results*

At the end of this project, we have detailed the implementation process of our custom code, mirroring the approach used in the original study. This included the development of an error function based on the symmetric definition of h(n). However, we encountered a challenge as our optimization problem turned out to be non-convex, making it unsolvable with our methods. Consequently, we adopted the coefficients detailed in the original paper to construct our scaling and wavelet functions, as illustrated in Figure 11 and Figure 12. For our analysis, we utilized a publicly available ECG dataset from GitHub, the link to which is cited in our references("ECGData", 2016).

To simulate a real-world scenario, we added White Gaussian Noise (WGN) with an amplitude of 0.03V to the original ECG signal. We then applied the denoising algorithm, as shown in Figure 1, using a single decomposition level. The effectiveness of our denoising process was evaluated by comparing it with results obtained using standard db4 and Sym4 wavelets. Figure 12 presents a comprehensive comparison, showcasing the original ECG signal, the signal with added noise, and the signals denoised using db4, Sym4, and our customized wavelet, respectively(Figure 13).

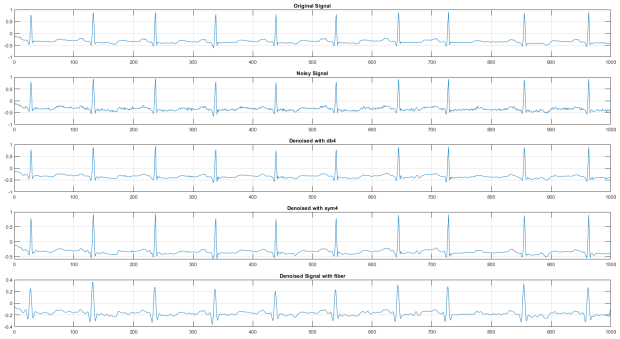

Figure 13: Our Denoising Results

5.2.5. *Conclusion*

The Fibr wavelet introduced in this paper, designed through an optimization process to mimic an ideal filter, surpassed the commonly used db4 and Sym4 wavelets in denoising effectiveness, particularly for ECG signals. When White Gaussian Noise was added to the signal, the denoising achieved with the Fibr

wavelet consistently yielded a higher average SNR and lower MSE. This superior performance in noise reduction was also evident in cases involving atrial fibrillation (AF) signals.

References

Almahamdy, M., & Riley, H. (2014). Performance study of different denoising methods for ecg signals. *Procedia Computer Science*, *37*, 325–332. https://doi.org/10.1016/j.procs.2014.08.048

AlMahamdy, M., & Riley, H. B. (2014). Performance study of different denoising methods for ecg signals [The 5th International Conference on Emerging Ubiquitous Systems and Pervasive Networks (EUSPN-2014)/ The 4th International Conference on Current and Future Trends of Information and Communication Technologies in Healthcare (ICTH 2014)/ Affiliated Workshops]. *Procedia Computer Science*, *37*, 325–332. https://doi.org/https://doi.org/10.1016/j.procs.2014.08.048

Ecgdata. (2016). https://raw.githubusercontent.com/mathworks/physionet_ECG_data/main/ECGData.zip

Mallat, S. (1989). A theory for multiresolution signal decomposition: The wavelet representation. *IEEE Transactions on Pattern Analysis and Machine Intelligence*, *11*(7), 674–693. https://doi.org/10.1109/34.192463

Marzog, H. A., Abd, H. J., & Yonis, A. (2022). Noise removal of ecg signal using multi-techniques. *2022 IEEE Integrated STEM Education Conference (ISEC)*, 397–403. https://doi.org/10.1109/ISEC54952.2022.10025094

Schomer, F. L., Donald L.; da Silva. (2011). *Niedermeyer's electroencephalography: Basic principles, clinical applications, and related fields*. Lippincott Williams Wilkins (LWW).

Shapiro, J. (1993). Embedded image coding using zerotrees of wavelet coefficients. *IEEE Transactions on Signal Processing*, *41*(12), 3445–3462. https://doi.org/10.1109/78.258085

Shi, F. (2022). A review of noise removal techniques in ecg signals. *2022 IEEE Conference on Telecommunications, Optics and Computer Science (TOCS)*, 237–240. https://doi.org/10.1109/TOCS56154.2022.10015982

Stridh, M., & Sörnmo, L. (2001). Spatiotemporal qrst cancellation techniques for analysis of atrial fibrillation. *IEEE transactions on biomedical engineering*, *48*, 105–11. https://doi.org/10.1109/10.900266

6. Code Appendix

clc; clear;

l = 8; w1 = linspace(0, pi/2,100); w2 = linspace(pi/2, pi, 100); cosine$_w$1 $= cos((0 : l-1)' * w1)$; $cosine_w2 = cos((0 : l-1)' * w2)$; $sine_w1 = sin((0 : l-1)' * w1)$; $sine_w2 = sin((0 : l-1)' * w2)$;

h$_n$ $= optimvar('h'_n, l)$; $squre_{hnw}1 = ((h'_n * cosine_w1).^2 + (h'_n * sine_w1).^2)/2$; $squre_{hnw}2 = ((h'_n * cosine_w2).^2 + (h'_n * sine_w2).^2)/2$; $objec = sum(1 - squre_{hnw}1) + sum(squre_{hnw}2)$;

prob = optimproblem('Objective',objec); prob.Constraints.cons1 = sum(h$_n$) $== sqrt(2)$; $prob.Constraints.cons2 = h_n(1) == h_n(8)$; $prob.Constraints.cons3 = h_n(2) == h_n(7)$; $prob.Constraints.cons4 = h_n(3) == h_n(6)$; $prob.Constraints.cons5 = h_n(4) == h_n(5)$;

problem = prob2struct(prob); [x,fval] = quadprog(problem);

clc; clear;

h = [0.001590, -0.056193, 0.056736, 0.493436, 0.493436, 0.056736, -0.056193, 0.001590];

h = h / sum(h);

phi = zeros(1, 2048); phi(floor(length(phi)/2)) = 1;

iterations = 8; for i = 1:iterations phi = conv(phi, h); phi = phi / sum(phi); end

midpoint = floor(length(phi)/2); range = (midpoint-20):(midpoint+20);

figure(1); plot(range, phi(range)); title('Scaling Function'); grid on;

g = zeros(1, length(h)); for n = 1:length(h) g(n) = (-1)$^n * h(length(h) - n + 1); end$

psi = [1]; for i = 1:iterations psi = conv(psi, g); psi = psi / norm(psi, 2); end

figure(2); plot(psi); title('Wavelet Function'); grid on;

save("..ϕ.mat", "phi"); save("..ψ.mat", "psi");

clc; clear;

filename = 'ECGData.mat'; loadedData = load(filename);

disp('Variables loaded from the file:'); disp(fieldnames(loadedData));

data = loadedData.ECGData.Data; sampleToPlot = data(1, 1:1000);

figure(1); plot(sampleToPlot); title('ECG Signal'); xlabel('Time'); ylabel('value'); ylim([-1,2]); grid on;

noiseLevel = 0.03; noisySignal = sampleToPlot + randn(size(sampleToPlot)) * noiseLevel;

load("..ϕ.mat"); load("..ψ.mat")

approximation = downsample(conv(noisySignal, phi, 'same'), 2); detail = downsample(conv(noisySignal, psi, 'same'), 2);

threshold = sqrt(2 * log(length(detail))); detail(abs(detail) < threshold) = 0;

reconPhi = flip(phi); reconPsi = flip(psi); Draft

upsampledApproximation = conv(upsample(approximation, 2), reconPhi, 'same'); upsampledDetail = conv(upsample(detail, 2), reconPsi, 'same');

denoisedSignal = upsampledApproximation + upsampledDetail;

[denoisedSignal$_db4$, ,] = $wdenoise(noisySignal, 5, 'Wavelet', 'db4')$;

[denoisedSignal$_sym4$, ,] = $wdenoise(noisySignal, 5, 'Wavelet', 'sym4')$;

figure(2); subplot(5,1,1); plot(sampleToPlot); title('Original Signal'); grid on;

subplot(5,1,2); plot(noisySignal); title('Noisy Signal'); grid on;

subplot(5,1,3); plot(denoisedSignal$_db4$); $title('Denoisedwithdb4'); gridon$;

subplot(5,1,4); plot(denoisedSignal$_sym4$); $title('Denoisedwithsym4'); gridon$;

subplot(5,1,5); plot(denoisedSignal); title('Denoised Signal with fiber'); grid on;